

# Discrimination of Redox-Responsible Biomolecules by a Single Molecular Sensor

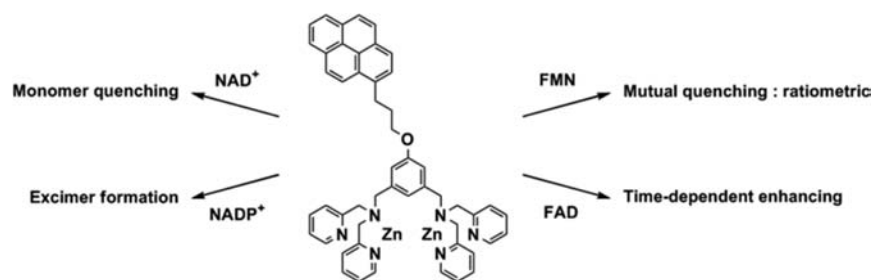
Jinrok Oh and Jong-In Hong\*

Department of Chemistry, College of Natural Sciences, Seoul National University,  
Seoul 151-747, Korea

jihong@snu.ac.kr

Received January 15, 2013

## ABSTRACT



A new application of a fluorescent sensor (PyDPA) for the discrimination of redox-responsible molecules is reported. Nicotinamide adenine dinucleotide/nicotinamide adenine dinucleotide phosphate ( $\text{NAD}^+/\text{NADP}^+$ ) and flavin mononucleotide/flavin adenine dinucleotide (FMN/FAD) were differentiated by means of ratiometric fluorescence change from excimer–monomer equilibrium and time-dependent fluorescence change, respectively.

Redox reactions are ubiquitous in biological systems because they are involved in protein regulation, oxidative phosphorylation, and metabolic reactions.<sup>1</sup> Redox-responsible functional groups, such as N-alkyl- $\beta$ -nicotinamide and the isoalloxazine moiety, are involved in biological redox reactions.

Nicotinamide adenine dinucleotide ( $\text{NAD}^+$ ) and nicotinamide adenine dinucleotide phosphate ( $\text{NADP}^+$ ) contain  $\beta$ -nicotinamide, which is responsible for hydride-transfer reactions. In particular,  $\text{NAD}^+$  and  $\text{NADP}^+$  are known to be extensively involved in oxidative reactions and reductive reactions, respectively.<sup>1</sup> Flavin mononucleotide (FMN), flavin adenine dinucleotide (FAD), and riboflavin have the isoalloxazine moiety in common, and they serve as either electron acceptors in the oxidized form or as electron donors in the reduced form. As a prosthetic group in flavoproteins, they are involved in metabolic reactions and the redox reactions of electron transport chains.<sup>2</sup> The most intriguing feature about these molecules is the

relationship between their structures (Figure 1) and their roles. For example,  $\text{NADP}^+$  has the same structure as that of  $\text{NAD}^+$  except for an additional phosphate group at the 2' position of the ribose ring connected to the adenine moiety. The slight structural difference between  $\text{NAD}^+$  and  $\text{NADP}^+$  leads to a significant difference in their roles:  $\text{NAD}^+$  for oxidative and  $\text{NADP}^+$  for reductive reactions.

Capillary electrophoresis (CE) techniques have been developed for the detection of nicotinamide derivatives<sup>3</sup> and flavins.<sup>4</sup> However, CE cannot be used for the real-time or in vivo detection of those redox-responsible biomolecules. It is known that the adenine unit of FAD significantly decreases the fluorescence of isoalloxazine by an intramolecular photo-induced electron transfer (PeT) quenching mechanism,<sup>5</sup> which has attracted considerable attention in the detection and discrimination of flavins using fluorescence methods.

Recently, we successfully demonstrated that sensors derived from the bis(Zn(II)-DPA) complex (DPA, dipicolylamine) could detect phosphate-containing molecules (Figure 2):

(1) Berg, J. M.; Tymoczko, J. L.; Stryer, L. *Biochemistry*; W. H. Freeman and Company: New York, 2006.

(2) (a) Walsh, C. *Acc. Chem. Res.* **1980**, *13*, 148. (b) Bruice, T. C. *Acc. Chem. Res.* **1980**, *13*, 256. (c) Massey, V. *Biochem. Soc. Trans.* **2000**, *28*, 283.

(3) Soga, T.; Igarashi, K.; Ito, C.; Mizobuchi, K.; Zimmermann, H. P.; Tomita, M. *Anal. Chem.* **2009**, *81*, 6165.

(4) Britz-McKibbin, P.; Markuszewski, M. J.; Iyanagi, T.; Matsuda, K.; Nishioka, T.; Terabe, S. *Anal. Biochem.* **2003**, *313*, 89.

(5) Sarma, R. H.; Dannies, P.; Kaplan, N. O. *Biochemistry* **1968**, *7*, 4359.

**PTZ-DPA** [PTZ-DPA consists of bis(Zn(II)-DPA) and phenothiazine (PTZ)] was utilized to discriminate between FAD and FMN. FAD was detected by the fluorescence increase through the catalytic self-lysis of FAD into cyclic FMN (cFMN) and adenosine monophosphate (AMP), while the fluorescence of FMN was significantly decreased by PeT from the PTZ in **PTZ-DPA** to the isoalloxazine group.<sup>6</sup> **PyDPA** shows selective excimer-based recognition of ppGpp which contains two pyrophosphate groups.<sup>7</sup> These results inspired us to study further the ability of **PyDPA** to discriminate between redox-responsible molecules.

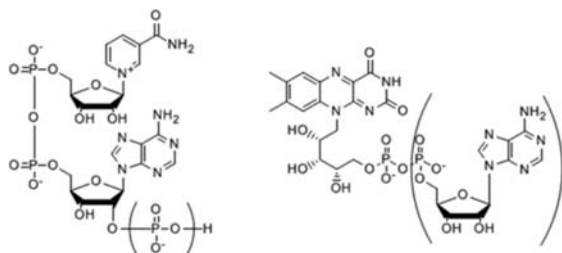


**Figure 1.** Chemical structures of NAD(P)<sup>+</sup> (left) and FMN(FAD) (right).

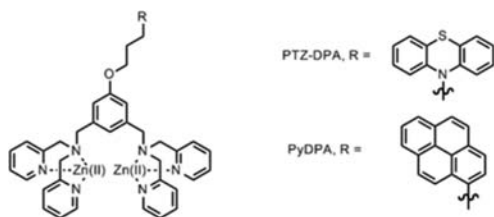


**Figure 2.** Chemical structures of **PyDPA** and **PTZ-DPA**.

First, we developed a new strategy for the synthesis of **PyDPA**, as shown in Scheme S1. The previously reported synthetic route employs several low-yielding steps such as metal–halogen exchange followed by transition metal-free aliphatic halide substitution, and nucleophilic phenol substitution. The new synthesis replaced these two low-yielding steps by a malonic acid Knoevenagel condensation-catalytic hydrogenation-reduction sequence, and a Mitsunobu reaction, respectively. Although the number of steps is increased, overall yield is greatly improved. Notably, single chromatographic separation at the final stage is sufficient to produce pure **PyDPA** (for a detailed procedure and characterization, see Supporting Information).

We conducted fluorescence titration experiments to investigate the possibility of discrimination between

NAD<sup>+</sup> and NADP in 1 mM HEPES buffer solution using **PyDPA**. Because NADP<sup>+</sup> has an additional phosphate group, we expected that only NADP<sup>+</sup> could induce excimer formation. As depicted in Figure 3, the addition of either NAD<sup>+</sup> or NADP<sup>+</sup> resulted in a decrease in monomeric fluorescence of pyrene, and concomitantly, only NADP<sup>+</sup> showed increased excimer emission centered at 470 nm and the shape of excimer emission was the same as reported previously.<sup>7,8</sup> This result indicates that it is possible to discriminate NADP<sup>+</sup> from NAD<sup>+</sup> by the fluorometric method.

What would cause the decrease in the monomeric pyrene emission upon the addition of either NAD<sup>+</sup> or NADP<sup>+</sup>? In a previously reported screening test, binding of adenosine derivatives to **PyDPA** resulted in enhancement of the monomeric pyrene emission;<sup>7</sup> thus, the nicotinamide moiety seems to be responsible for emission quenching of pyrene. The underlying quenching mechanism was determined by performing electrochemical studies using **5** (Scheme S1) and **BnN** (Scheme S2) as model compounds of pyrene and nicotinamide, respectively. Reduction potentials of **5** and **BnN** were estimated to be −3.52 and −3.75 eV from the vacuum level (Table S1). This slightly higher lowest unoccupied molecular orbital (LUMO) level of pyrene (~0.2 eV) suggests that oxidative PeT quenching from the excited pyrene to NAD<sup>+</sup> is possible. On the other hand, the

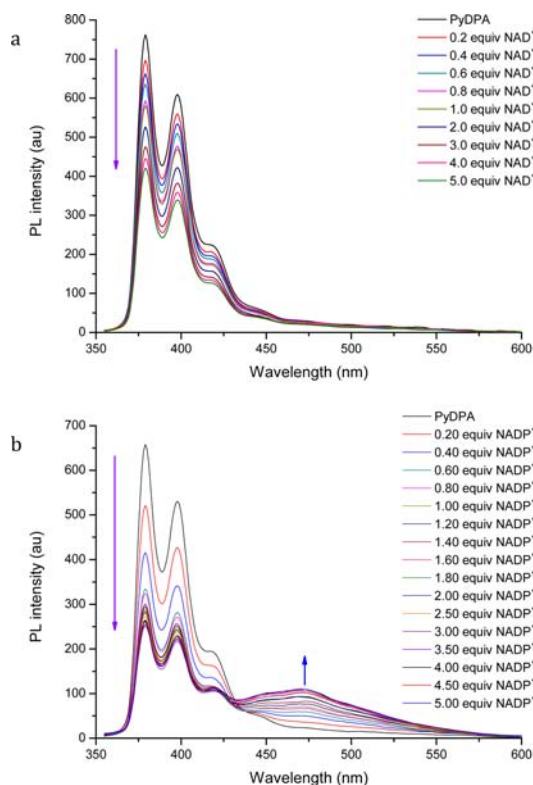


**Figure 3.** Fluorescence spectral changes upon the addition of either (a) NAD<sup>+</sup> or (b) NADP<sup>+</sup> in the presence of 20 μM **PyDPA** in 1 mM HEPES buffer solution (0.1% DMSO, pH = 7.40), λ<sub>ex</sub> = 344 nm.

(6) Rhee, H.-W.; Choi, S. J.; Yoo, S. H.; Jang, Y. O.; Park, H. H.; Pinto, R. M.; Cameselle, J. C.; Sandoval, F. J.; Roje, S.; Han, K.; Chung, D. S.; Suh, J.; Hong, J.-I. *J. Am. Chem. Soc.* **2009**, *131*, 10107.

(7) Rhee, H.-W.; Lee, C.-R.; Cho, S.-H.; Song, M.-R.; Cashel, M.; Choy, H. E.; Seok, Y. J.; Hong, J.-I. *J. Am. Chem. Soc.* **2008**, *130*, 784.

highest occupied molecular orbitals (HOMOs) of **5** and **BnN** were estimated to be  $-6.87$  and  $-8.17$  eV, respectively. However, the calculated HOMO level of  $\text{NAD}^+$  is not expected to be in the nicotinamide core<sup>9</sup> and the large energy level difference (1.3 eV) is undesirable for electron transfer.<sup>10</sup> Therefore, the D-type-PeT (electron transfer from the excited pyrene to nicotinamide species) mechanism seems most plausible for quenching.

Further study on the binding between **PyDPA** and  $\text{NAD(P)}^+$  was performed. In the case of  $\text{NAD}^+$ , the fluorescence spectral changes at 398 nm fitted well with a one-to-one binding equilibrium, and its binding constant ( $K_a$ ) was estimated to be  $4.4 \times 10^4 \text{ M}^{-1}$ , which is similar to the binding affinity toward monohydrogen phosphate.<sup>11</sup>  $\text{NADP}^+$  showed more efficient quenching of the emission of monomeric pyrene than did  $\text{NAD}^+$ , and it does not follow a one-to-one binding equilibrium. Interestingly, the emission changes of **PyDPA** when a 2-fold concentration of  $\text{NADP}^+$  ( $R^2 = 0.983$ ) is used indicates that **PyDPA** interacts with  $\text{NADP}^+$  with a 2:1 binding stoichiometry via coordination with diphosphate and phosphate moieties; the two corresponding binding constants were assumed to be very similar. Job's plot analysis also supports a 2:1 binding stoichiometry. The apparent  $K_a$  of  $\text{NADP}^+$  was estimated to be  $3.7 \times 10^5 \text{ M}^{-1}$ , which is about 8 times larger than that of  $\text{NAD}^+$ . One intriguing observation is that the pyrene dimer formed in the 2:1 complex was not destroyed upon addition of even large amounts of  $\text{NADP}^+$  during the titration experiment. This is completely different from the binding of **PyDPA** to ppGpp, in which the excimer emission decreased at a high level of ppGpp.<sup>7,12</sup> This saturation behavior and ratiometric property toward  $\text{NADP}^+$  would be advantageous in the selective sensing of  $\text{NADP}^+$ , while ppGpp shows concentration-dependent pyrene excimer emission, showing the highest excimer emission at optimal guest concentration. The fact that **PyDPA**- $\text{NADP}^+$  complexation exhibits an increased  $K_a$  compared to that of **PyDPA** binding with  $\text{NAD}^+$  and maintains the pyrene dimeric structure even at high concentrations of  $\text{NADP}^+$  can be understood in terms of the cooperative effect of the aromatic groups involved in the termolecular complexation.<sup>13</sup>

Next, we wondered if **PyDPA** can discriminate flavin species by taking advantage of isoalloxazine's fluorescence. A fluorescence titration experiment for FMN revealed that the monomeric emission of **PyDPA** was greatly decreased, while FMN emission centered at 526 nm was

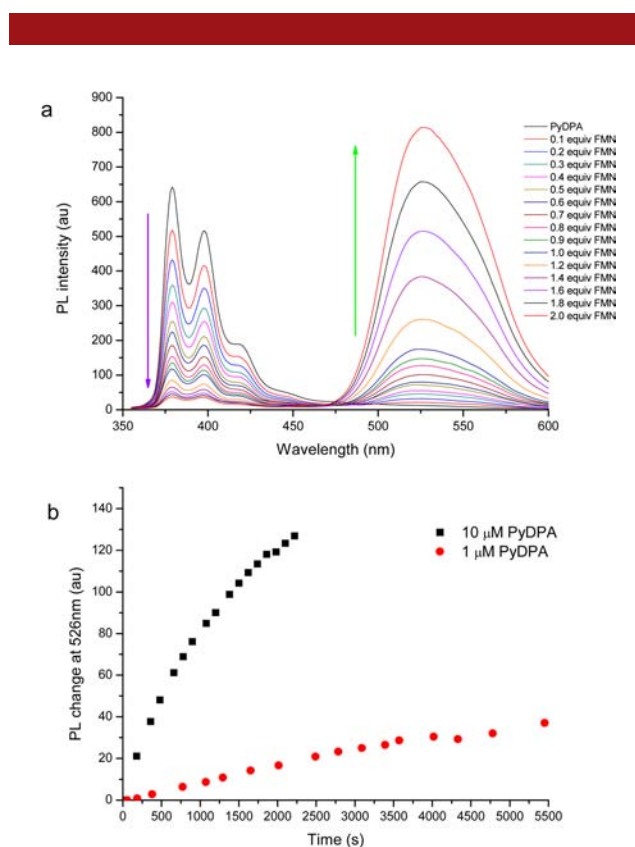


**Figure 4.** (a) Fluorescence spectral change upon addition of FMN in the presence of  $20 \mu\text{M}$  **PyDPA**. (b) Fluorescence intensity change at 526 nm with time in the presence of  $15 \mu\text{M}$  FAD and either  $1 \mu\text{M}$  (red circle) or  $10 \mu\text{M}$  (black square) of **PyDPA**. In both cases, experiments were performed in  $1 \text{ mM}$  HEPES buffer solution ( $\text{pH} = 7.40$ ), excitation =  $344 \text{ nm}$ .

enhanced, which may indicate that fluorescence resonance energy transfer (FRET) between the two fluorophores (pyrene and isoalloxazine) occurs (Figure 4a). However, the normalized excitation spectra of FMN did not differ, regardless of **PyDPA** presence, which implies that no efficient FRET between **PyDPA** and FMN takes place (Figure S8). Also, addition of pyrophosphate<sup>14</sup> resulted in a great enhancement in the emission intensity of both **PyDPA** and FMN (Figure S9). These results suggest that there is extensive mutual quenching between **PyDPA** and FMN. Interestingly, however, we were able to detect green fluorescence from isoalloxazine in a 1:1 mixture of **PyDPA** and FMN under 365 nm UV light.

The quenching mechanism of **PyDPA** by FMN (and vice versa) was also studied by the electrochemical method. Reduction potentials of both pyrene and FMN were measured to be  $-3.52 \text{ eV}$ , as shown in Table S1, indicating that reversible electron transfer between the two LUMOs of the fluorophores is possible. However, the estimated HOMOs of pyrene and FMN are at  $-6.87$  and  $-5.92 \text{ eV}$ , respectively, from the vacuum level. These data suggest that efficient A-type PeT [electron transfer from the

(8) Schazmann, B.; Alhashimy, N.; Diamond, D. *J. Am. Chem. Soc.* **2006**, *128*, 8607.

(9) The HOMO of the nicotininium core is estimated to be  $-8.17 \text{ eV}$ . The value is estimated from its reduction potential and optical band gap,  $4.4 \text{ eV}$ , corresponding to the absorption onset point,  $280 \text{ nm}$ .

(10) Siders, P.; Marcus, R. A. *J. Am. Chem. Soc.* **1981**, *103*, 748.

(11) Han, M. S.; Kim, D. H. *Angew. Chem., Int. Ed.* **2002**, *41*, 3809.

(12) From the energetic point of view, these phenomena might originate from the similar interaction strengths of bisZn(DPA)-phosphate and pyrene-pyrene in water. This would result in stabilization of the equilibrium state. However, in the ppGpp case, the binding strength of bisZn(DPA)-pyrophosphate overwhelms that of pyrene-pyrene, and thus, equilibrium would be shifted toward destroying the dimeric form of pyrenes at high ppGpp concentration.

(13) Kool, E. T. *Chem. Rev.* **1997**, *97*, 1473.

(14) Because pyrophosphate has a greater binding affinity toward the 1,3-bis(Zn-DPA) moiety than FMN, addition of pyrophosphate eliminates the weaker interaction between **PyDPA** and FMN.

HOMO of FMN to the lower singly occupied molecular orbital (SOMO) of excited **PyDPA**] quenching occurred. From the relative energy level distribution, it is expected that **PyDPA** is extensively quenched by FMN, while FMN itself is partially quenched, which is exactly what is observed.

Our first attempt to rationalize the fluorescence changes of **PyDPA** with respect to FMN concentration failed under the assumption of a 1:1 binding mode. There are two possible explanations for this: (1) more than one quenching pathway is involved and (2) multiple binding modes are involved. A Stern–Volmer plot of **PyDPA** (Figure S6), in the presence of FMN as a quencher, showed two different proportional coefficients. This implies that there are two major quenching pathways: PeT quenching between isoalloxazine and pyrene, which is supported by the electrochemical data; and absorption sharing of **PyDPA** and FMN. Job's plot reveals a 2:1 binding stoichiometry between **PyDPA** and FMN (Figure S7), presumably through coordination with phosphate and imide moieties.<sup>14</sup> On the basis of these results and an assumption,<sup>15</sup> the **PyDPA** spectral change was successfully rationalized with respect to FMN concentration. The apparent association constant was estimated to be  $1.93 \times 10^5 \text{ M}^{-1}$ , and the quenching efficiency of FMN to **PyDPA** was estimated to be 1.0 (Figure S5), which is consistent with the results of other experiments, such as the addition of pyrophosphate to the **PyDPA**-FMN combination (Figure S9) and the excitation spectra of FMN (Figure S8).

Because the catalytic group for the self-lysis of FAD [bisZn(II)DPA] is exactly the same in **PyDPA** as in **PTZ-DPA**, **PyDPA** is also expected to catalyze the lysis of FAD into cFMN and AMP and show a similar fluorescence enhancing behavior at 526 nm (which is exactly the emission of isoalloxazine ring) with time as in the case of **PTZ-DPA**

(15) As in the case of binding between **PyDPA** and  $\text{NADP}^+$ , the two binding constants between **PyDPA** and FMN are assumed to be similar.

catalysis (Figure 4b).<sup>6</sup> This fluorescence change also agrees well with pseudo-first-order kinetics, with an apparent rate constant of  $70 \text{ s}^{-1}$ . These results indicate that **PyDPA** can discriminate between riboflavin, FMN, and FAD with respect to (time-course) fluorescence spectral change: FMN is significantly quenched by the addition of a large amount of **PyDPA**; FAD is detected by a gradual increase in the fluorescence intensity of isoalloxazine with time upon addition of **PyDPA**; and finally, the fluorescence of riboflavin is not altered by **PyDPA**.

In conclusion, we developed a new synthetic strategy for the production of **PyDPA** and investigated its further use in the discrimination of redox-related biomolecules.  $\text{NAD}^+$  and  $\text{NADP}^+$  were distinguished by the presence or absence of the excimer emission of **PyDPA**. FMN and FAD were differentiated by means of the quenching of FMN emission and the time-dependent fluorescence enhancement, respectively. Interesting features of sensing, such as the cooperative effect of the aromatic groups involved in the **PyDPA**- $\text{NADP}^+$  complexation for maintaining the pyrene dimeric structure or absorption sharing of **PyDPA** and FMN in the detection of FMN, may give insight in designing sensors and the analysis of complicated emission profiles.

**Acknowledgment.** This work was supported by an NRF grant funded by the MEST (Grant No. 2012-0000159). J.O. was supported by the Hi Seoul Science/Humanities Fellowship from the Seoul Scholarship Foundation.

**Supporting Information Available.** Synthesis details, experimental details, calculation basis, fitting results, additional spectroscopic data, and electrochemical data. This material is available free of charge via the Internet at <http://pubs.acs.org>.

The authors declare no competing financial interest.